

Diagnosis GLY120 Antigen for the Blood and Breast Cancers Using Graphene Nanosheet

Reza Sabbaghi-Nadooshan* and Mojtaba Siasar Karbasaki

Department of Electrical Engineering, Central Tehran Branch, Islamic Azad University, Tehran, Iran.

(*) Corresponding author: r_sabbaghi@iauctb.ac.ir
(Received: 16 January 2014 and Accepted: 08 February 2017)

Abstract

The current study designed and simulated graphene nanosensors for detection of GLY120 tumor-associated carbohydrate antigens. Graphene is a two-dimensional nanosheet that offers a high surface-to-volume ratio and high mobility which increases its sensitivity as a graphene sensor over that of other nanoparticles. The current study simulated graphene sensors with and without GLY120 tumor markers and compared the two conditions. GLY120 tumor-associated antigens are present in blood and breast tissue. When GLY120 was attached to the graphene sheet, the Fermi energy, total energy, potential energy, band structure energy and electron kinetic energy of the nanosheet changed. It was then possible to determine the difference in the $V_D - I_D$ curves in each state.

Keywords: Diagnosis, Cancer, GLY120 Antigen, Graphene.

1. INTRODUCTION

The development of sensors, especially in biosensors, has been notable. Nanotechnology is a developing field [1, 2], for which one of the most important applications is in sensors. Traditional nanosensors have been based on carbon nanotubes (CNTs) [3, 4]. With the development of graphene from graphite [5], researchers have sought to find uses for this type of nanosheet.

Graphene is a two-dimensional nanoparticle consisting of bonded carbon atoms in a hexagonal lattice with unique properties [6]. It is essentially a single atomic layer of graphite with exceptional electronic properties such as a zero bandgap, carrier mobility exceeding $15000 \text{ cm}^2\text{V}^{-1}\text{s}^{-1}$ at room temperature, ballistic transport of carriers similar to CNTs, a massless Dirac electronic structure, anomalous quantum Hall effects and extraordinarily high thermal conductivity, stiffness and strength [7, 8]. Another unique attribute is its high surface-to-volume ratio [9], which makes possible its use for highly sensitive sensors [10, 11].

Graphene is used in biosensors based on graphene for detection of various biomolecules [12-14] and in graphene-based nanomedicine applications [15-17]. The current study designed and simulated graphene nanosensors as biosensors to detect GLY120 tumor-associated carbohydrate antigen. This antigen is found in blood and breast tissue. The results demonstrate that adding GLY120 to the surface of a graphene nanosheet alters the properties of the graphene (Fermi energy, energy band structure, total energy, potential energy and electron kinetic energy). The changes in the graphene properties cause changes in the $V_D - I_D$ characteristics in the presence of GLY120. The simulation assumes that the proposed sensor is functionalized and only specific molecules are attracted to it.

2. PROPOSED METHOD

A graphene electrode was initially designed using a gold electrode, which offers greater conductivity than other atoms [18]. To study the effect of the

presence of GLY120 on the graphene channel and sensor characteristics, the sensor structure was simulated with the graphene electrode without other molecules on the graphene sheet channel. The electrical parameters for the graphene sheet (Fermi energy, total energy, potential energy, band structure energy and electron kinetic energy) were obtained. Next, the tumor marker was attached to the graphene and the simulation was repeated.

It was necessary to obtain a parameter such as electron charge or force between electrons; thus, the capacitance of the sheet as a major parameter was calculated. The graphene sheet was assumed to have three series capacitances. Using the electron charge and force between electrons obtained through the simulation, the series capacitances were calculated. Next, the total capacitance (C_G) was calculated (Fig. 1). By using the capacitance of graphene FET models, the changes in $V_D - I_D$ characteristics in presence of GLY120 were determined.

To obtain the properties of the graphene and calculate the capacitance, the software Virtual Nanolab was used. This software is powerful in simulating on a nanoscale. Virtual NanoLab is a graphical interface that provides a group of modeling tools for use in setting up, investigating and studying nanoscale structures such as molecules and bulk and two-probe systems [19].

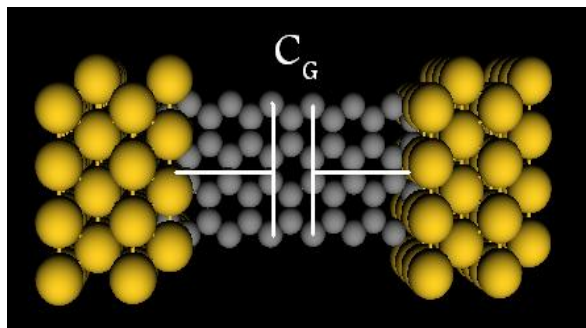


Figure 1. Schematic of CG capacitor in graphene sheet.

2.1. Graphene Fet Models

2.1.1. Meric's Model

Meric's model [20] was used to design the graphene nanosensor [20]. This model is a transistor consisting of two gates and a graphene channel (Fig. 2).

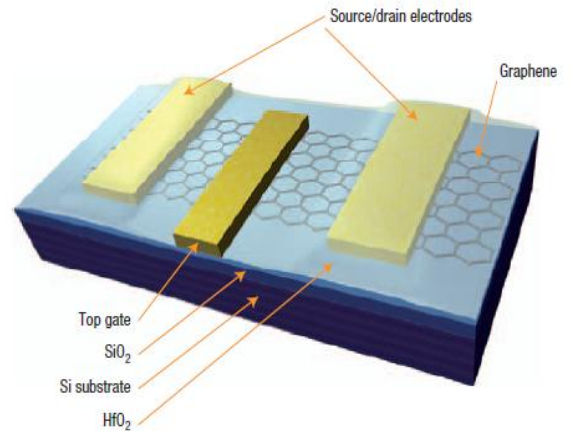


Figure 2. Schematic of a graphene FET on a Si/SiO substrate with a heavily doped Si wafer acting as a back gate and a gold top gate.

In the meric's method, I_D is obtained as:

$$I_D = \frac{Zq\mu_0}{L} \frac{\int_0^{V_{ds}} n(v)dv}{1 + \frac{\mu_0}{LV_{sad}} |V_{ds}|} \quad (1)$$

where Z is top gate width, μ_0 is channel mobility, L is top gate length, and $n(v)$ can be obtained by Eq. (2) [21].

$$n(V_{ds}) = n_0 \sqrt{1 + \left(\frac{C_{gst}}{n_0 q}\right)^2 (V_{gst} - V_{ds} - V_{th})^2} \quad (2)$$

and

$$\int_0^{V_{ds}} n(v)dv = \frac{n_0}{2\lambda} [\theta_{gs} - \theta_{gd} + \cosh \theta_{gs} \sinh \theta_{gs} - \cosh \theta_{gd} \sinh \theta_{gd}] \quad (3)$$

where:

$$\lambda = \frac{C_{gst}}{n_0 q} \quad (4)$$

$$\theta_{gd} = \sinh^{-1} \lambda (V_{gst} - V_{ds} - V_{th}) \quad (5)$$

$$\theta_{gs} = \sinh^{-1} \lambda (V_{gst} - V_{th}) \quad (6)$$

where the parameters are as below:

$$V_{gst} = 1/45$$

$$V_{sd} = 0V$$

the HfO₂ gate insulator (thickness of 15 nm)

back-gated GFETs with thick (300 nm) gate oxides [21].

2.1.2. GNRFET Model

The graphene nanoribbon FET (GNRFET) model [21, 22] can be used to investigate the properties of a graphene nanoribbon. In order to calculate drain current in GNRFET model, we can use following equations [22, 23]:

$$I_D = \frac{dQ}{dt} \quad (7)$$

$$I_D = \frac{nqL}{t} \quad (8)$$

$$I_D = nqv_d \quad (9)$$

v_d is given by [24]:

$$v_d = \frac{\xi\mu}{1 + \frac{\xi}{\xi_c}} \quad (10)$$

where ξ is the electric fields, μ is the mobility and ξ_c is the critical electric field. Then we have [23]:

$$v_d = \frac{\frac{v_{DS}\mu}{L}}{1 + \frac{\frac{L}{V_C}}{\frac{L}{V_C}}} = \frac{\mu}{L} \left[\frac{V_{DS}}{1 + \frac{V_{DS}}{V_C}} \right] \quad (11)$$

In Eq. (12), the relation between gate voltage and drain current is shown [22]:

$$\frac{E_F - E_C}{q} = \frac{V_G - V_T}{1 + \frac{C_Q}{C_C}} \quad (12)$$

where V_T is the threshold voltage, C_Q is the quantum capacitance and C_{OX} is the oxide capacitance. Finally critical voltage also can be rewritten as [23]:

$$V_C = \frac{L}{\mu} \left[\frac{K_B T}{4N_C \sqrt{\pi \hbar}} \left(\sqrt{\frac{q(V_g - V_T)}{K_B T (1 + \frac{C_Q}{C_{ins}})}} \right) \right] \quad (13)$$

The subbands have an effect on the band structure of the GNR, density of state (DOS), carrier concentration, carrier velocity, GNR current characteristics, carrier mobility and conductance of the GNR. Each subband has a different influence on carrier transport in the conduction and valence bands [23]. The I_D - V_D curves are plotted herein for the first, second and third subbands in the presence of the target chemical molecules on the graphene sheet.

3. SIMULATION RESULTS

3.1. Simulation Environment

The graphene was 1.4 nm in length and the tumor marker used was shown in Fig. 3(a). The first simulation did not contain a tumor marker on the graphene sheet. The second simulation contained the tumor marker (Fig. 3(b)) and allowed comparison of the results.

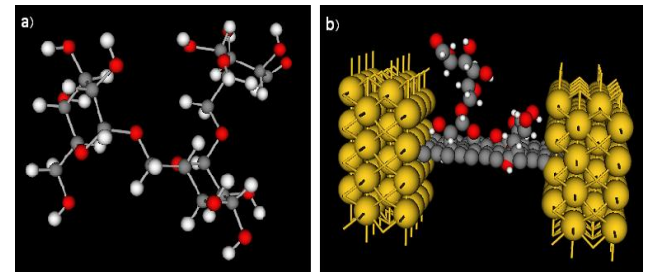


Figure 3. a) tumor marker b) graphene electrode in presence of tumor marker.

3.2. Results

After simulation, the capacitances were calculated and were shown in Table 1.

Table 1. Obtained capacitors values for C without any molecules and in reaction with tumor marker

No of molecule	0	1Tumor marker
C_G	7.93E-32	2.28E-31

When the tumor marker was attached to the graphene surface, the value of C_G

increased. The presence of the tumor marker increased the value of capacitance 10-fold greater than before. The I_D - V_D curves of both cases were shown in the Figure 4.

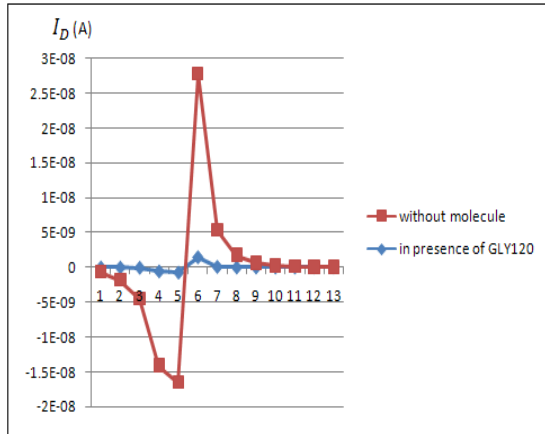


Figure 4. I_D - V_D curves without tumor markers (red curve) and in the presence of tumor marker (blue curve).

Fig. 4 showed that in the presence of GLY120 tumor marker, the maximum current of the graphene sheet decreased. Without the tumor marker, the maximum I_D was about 3 E^{-08} . With the addition of the GLY120 tumor marker, the maximum current was about 2 E^{-09} .

Using the formulations for GNR-FET (section 2), more trials were done to evaluate the sensitivity of the sheets. The results for I_D - V_{DS} at different gate voltages (0, 0.4, 0.8, 1.2, 1.6, 2 V) were derived for the first, second and third subbands.

Fig. 4 also showed that without the tumor marker, the current value at $v_d = 1 \text{ v}$ and $v_g = 2 \text{ v}$ for the first, second and third subbands was 1.25 E^{-3} , $>1.6 \text{ E}^{-3}$ and $>1.6 \text{ E}^{-3}$, respectively. Fig. 5 showed the results with the tumor marker and revealed the current values in the same drain and gate voltage for the first, second and third subbands to be 1 E^{-3} , 1.4 E^{-3} and $>1.6 \text{ E}^{-3}$, respectively. It was evident that when the tumor marker was attached to the graphene sheet, the drain current changed. This made it possible to design a graphene nanobiosensor that was very sensitive in reaction to the GLY120 tumor marker.

3.2.1. Properties of Nano-Graphene Sheet

This section examined the changes in the Fermi energy of the graphene when exposed to the GLY120 tumor marker. Fig. 5 showed that the Fermi energy for the graphene without a tumor marker was slightly more than 0.2 Ry and in presence of the tumor marker was slightly less than 0.2 Ry. The total energy, potential energy, band structure energy and electron kinetic energy were calculated in simulation and the results were shown in Fig. 6.

Fig. 7 showed that the final values for total, potential, band structure and kinetic energies of the graphene sheet without the attached molecule were 186000 ev, 186000 ev, 17200 ev and 103700 ev, respectively. When the tumor marker was attached, Fig. 7 showed that the final values for total, potential, band structure and kinetic energies of the graphene sheet without the attached molecule were 186000 ev, 186000 ev, 17200 ev and 103700 ev, respectively. When the tumor marker was attached, these parameters were evaluated as 182195 ev, 182195 ev, 16292 ev and 101404 ev, respectively.

4. CONCLUSION

This paper presented a novel method for investigation of the sensor properties of a biosensor that was created with a graphene nanosheet. The results showed that the current decreased when GLY120 tumor marker was absorbed onto the graphene sheet. Moreover, when the tumor marker attached to the graphene sheet, the values of the Fermi energy, total energy, potential energy, band structure and electron kinetic energy decreased. This study confirms that graphene can be used in a biosensor with high sensitivity.

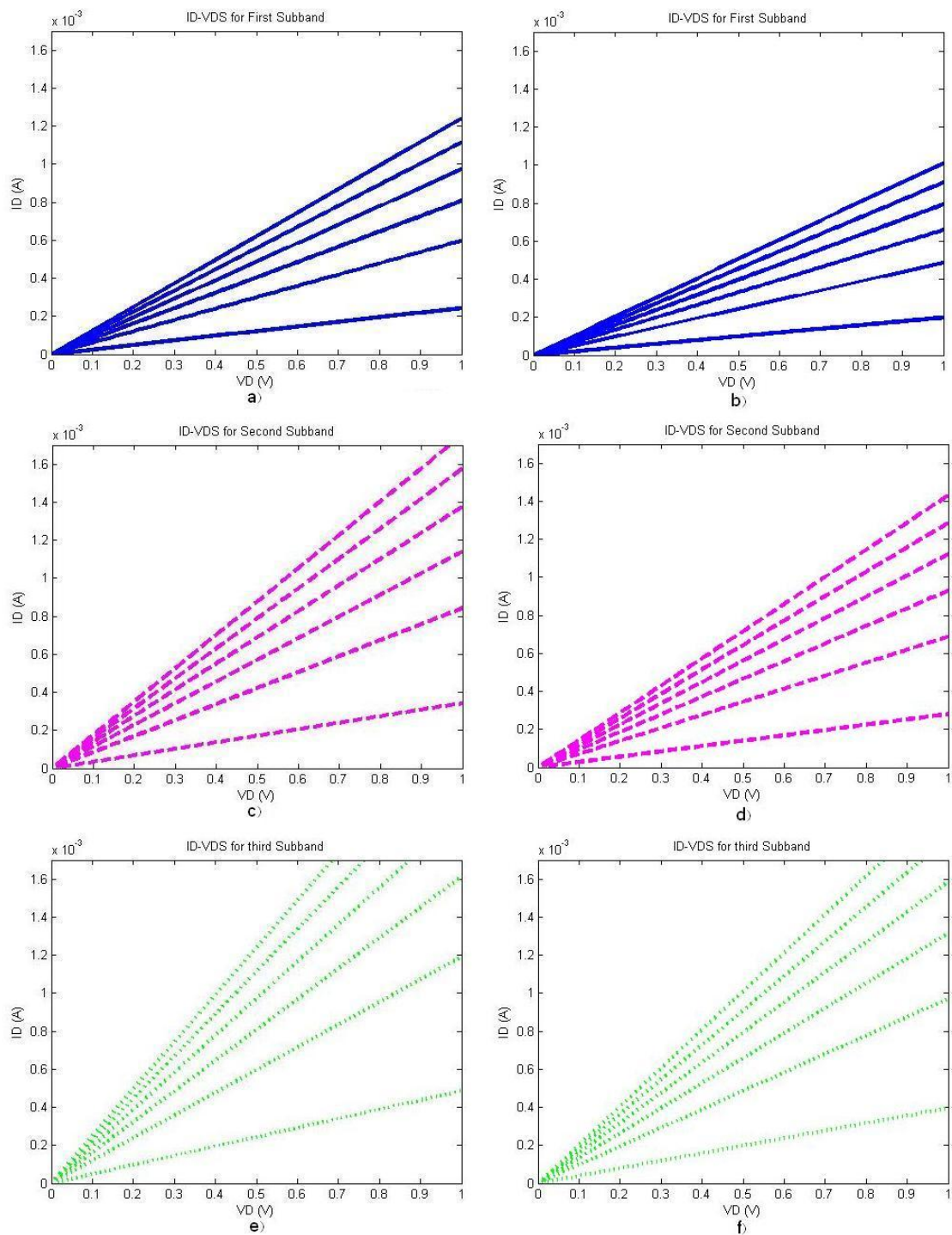


Figure 5. current versus voltage curves; a) without molecules for the first subband, b) in presence tumor marker for the first subband, c) without molecules for the second subband, d) in the presence tumor marker for the second subband, e) without molecules for the third subband f) in the presence tumor marker for the third subband.

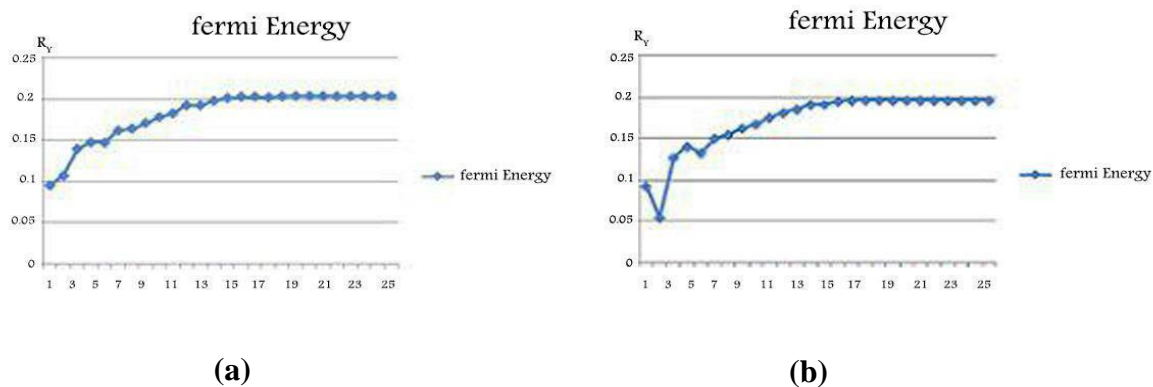


Figure 6. Changes in the Fermi energy a) without any molecule b) in the presence tumor marker molecule

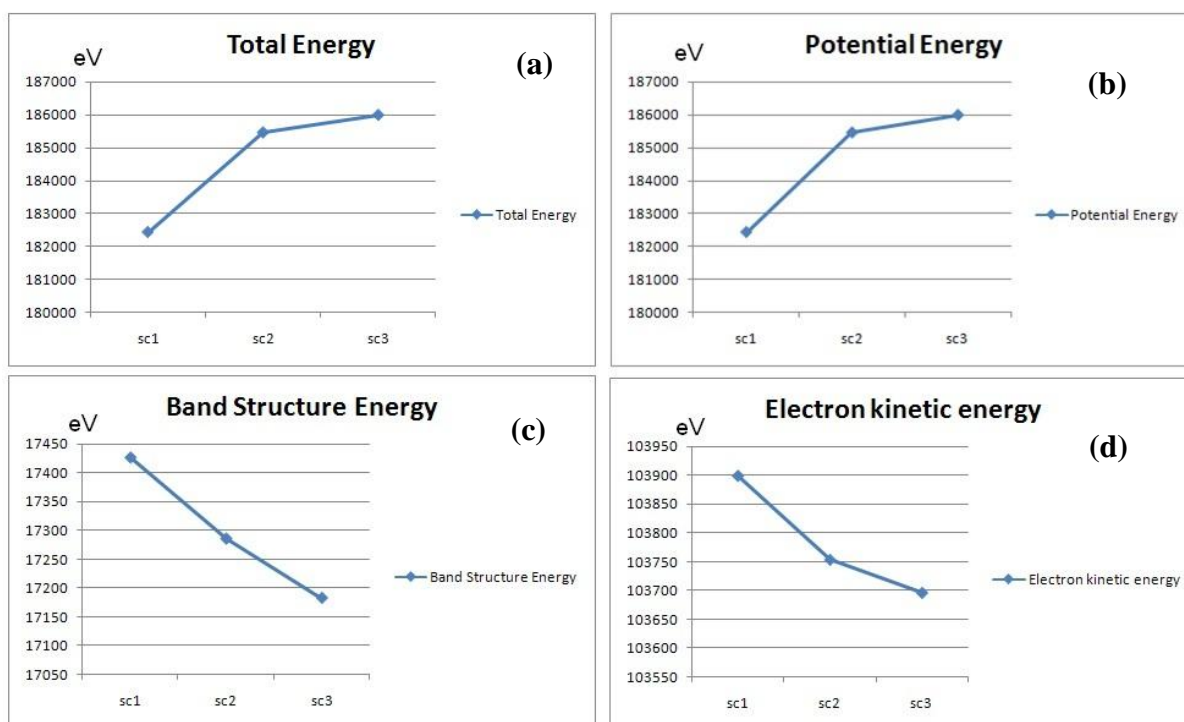


Figure 7. The value of the graphene sheet properties without any molecule on the graphene sheet a) Total energy b) Potential energy c) Band structure energy d) Electronic kinetic energy.

REFERENCES

1. Kianpour, M., Sabbaghi-Nadooshan, R. (2014). "Novel Design of n-bit Controllable Inverter by Quantum-dot Cellular Automata", *Int. J. Nanosci. Nanotechnol.*, 10: 117-126.
2. Kianpour, M., Sabbaghi-Nadooshan, R. (2013). "Optimized Design of Multiplexor by Quantum-dot Cellular Automata", *Int. J. Nanosci. Nanotechnol.*, 9: 15-24.
3. Zahedi, A. Kashaninia, A., Farokhi, F. (2011) "Carbon nanotube Field Effect Transistor-Based Gas Sensor for NH_3 Detection", *International Conference in Nanotechnology and Biosensors IPCBEE*, 25:54-58.

4. Zhang, Y., Liu, J., Li, X., Dou, J., Liu, W., He, Y., Zhu, C. (2001). "Study of gas sensor with carbon nanotube film on the substrate of porous silicon", *Proceedings of the 14th International Vacuum Microelectronics Conference*, 13-14.
5. Novoselov, K. S., Geim, A. K., Morozov, S. V., Jiang, D., Zhang, Y., Dubonos, S. V. (2004). "Electric field effect in atomically thin carbon films", *Science*, 306: 666-669.
6. Hill, E. W. (2011). "Graphene Sensors", *IEEE Sensors Journal*, 11: 3161-3170.
7. Guy, O. J., Castaing, A., Tehrani, Z., Doak, S. H. (2010). "Fabrication of Ultra-Sensitive Graphene Nano biosensors", *IEEE Sensors Conference*, 907-912.
8. Xu, Z. (2011). "Materials Physics and Applications of Graphene – Experiments", Edited S. Mikhailov, InTech Open, Croatia, p. 3.
9. Hwang, S., Cho, J. H., Lim, J., Kim, W. K., Shin, H., Choi, J. Y., Choi, J. H., Lee, S. Y., Kim, J. M., Kim, J.H., Lee, S., Jun, S. C. (2010). "Graphene based NO₂ gas sensor", *IEEE Nanotechnology Materials and Devices Conference*, 18-21.
10. Rivera, I. F., Joshi, R. K., Wang, J. (2010) Graphene-Based Ultra-Sensitive Gas Sensors, *IEEE Sensor*, 1534-1537.
11. Zhao, C. L., Qin, M., Huang, Q. A. (2011). "Humidity sensing properties of the sensor based on graphene oxide films with different dispersion concentrations", *IEEE Sensors*, 1-4.
12. Kou, R., Shao, Y. Y., Wang, D. H., Engelhard, M. H., Kwak, J. H., Wang, J., Viswanathan, V. V., Wang, C. M., Lin, Y. H., Wang, Y., Aksay, I. A., Liu, J. (2009). "Enhanced Activity and Stability of Pt Catalysts on Functionalized Graphene Sheets for Electrocatalytic Oxygen Reduction", *Electrochem. Commun.* 11: 954-957.
13. Yoo, E., Kim, J., Hosono, E., Zhou, H., Kudo, T., Honma, I. (2008). "Large reversible Li storage of graphene nanosheet families for use in rechargeable lithium ion batteries", *Nano Lett.* 8: 2277-2282.
14. Guo, S.R., Lin, J., Penchev, M., Yengel, E., Ghazinejad, M., Ozkan, C. S., Ozkan, M. (2011). "Label free DNA detection using large area graphene based field effect transistor biosensors", *Journal of Nanoscience and Nanotechnology*, 11: 5258-5263.
15. Tang, L., Wang, Y., Liu, Y., Li, J. (2011). "DNA-Directed Self-Assembly of Graphene Oxide with Applications to Ultrasensitive Oligonucleotide Assay", *ACS Nano*, 5: 3817-3822.
16. Zhang, M., Yin, B. C., Tan, W., Ye, B. C. (2011). "A versatile graphene-based fluorescence "on/off" switch for multiplex detection of various targets", *Biosensors and Bioelectronics*, 26: 3260-3265.
17. Ohno, Y., Maehashi, K., Matsumoto, K. (2010). "Label-Free Biosensors Based on Aptamer-Modified Graphene Field-Effect Transistors", *Journal of the American Chemical Society*, 132: 18012-18013
18. Zahedi, A., Kashaninia, A., Farokhi, F. (2011). "Carbon Nanotube Field Effect Transistor-Based Gas Sensor for NH₃ Detection", *International Conference on Nanotechnology and Biosensors*, 25:54-58.
19. Alzubi, F. G. (2008). "Atomistic Modeling of Elastic and Transport Properties of Carbon Nanotube", Master Thesis, Department of Physics and Astronomy Ball state University.
20. Meric, I., Han, M. Y., Young, A. F., Ozyilmaz, B., Kim, P., Shepard, K. L. (2008). "Current saturation in zero-bandgap, top-gated graphene field-effect transistors", *Nature Nanotechnology*, 3: 654-659.
21. Crowne, F. (2011). Classical Gradual-Channel Modeling of Graphene Field-Effect Transistors (FETs), Army Research Laboratory.
22. Xian, E. N. H. (2010). "Modeling and Performance Evaluation of Graphene Nanoribbon Field Effect Transistor", University Teknologi Malasia.
23. Redzuan, N. B. (2010). "Modeling of Subband Effects on Graphene Nanoribbon Field Effect Transistor Transport", University Teknologi Malaysia.
24. Shao, Y., Wang, J., Wu, H., Liu, J., Aksay, I. A., Lina, Y. (2010). "Graphene based electrochemical sensors and biosensors: A review", *Electroanalysis*, 22, 1027-1036.